

PROJECTED CONSTRAINTS ON THE COSMIC (SUPER)STRING TENSION WITH FUTURE GRAVITATIONAL WAVE DETECTION EXPERIMENTS

SOTIRIOS A. SANIDAS, RICHARD A. BATTYE AND BENJAMIN W. STAPPERS

Jodrell Bank Centre for Astrophysics, University of Manchester, Manchester, M13 9PL, United Kingdom;
sotiris.sanidas@gmail.com, rbattye@jb.man.ac.uk, ben.stappers@manchester.ac.uk

(Dated: September 26, 2018)
Draft version September 26, 2018

ABSTRACT

We present projected constraints on the cosmic string tension, $G\mu/c^2$, that could be achieved by future gravitational wave detection experiments and express our results as semi-analytic relations of the form $G\mu(\Omega_{\text{gw}}h^2)/c^2$, to allow for direct computation of the tension constraints for future experiments. These results can be applied to new constraints on $\Omega_{\text{gw}}h^2$ as they are imposed. Experiments operating in different frequency bands probe different parts of the gravitational wave spectrum of a cosmic string network and are sensitive to different uncertainties in the underlying cosmic string model parameters. We compute the gravitational wave spectra of cosmic string networks based on the one-scale model, covering all the parameter space accessed by each experiment which is strongly dependent on the birth scale of loops relative to the horizon, α . The upper limits on the string tension avoid any assumptions on the model parameters. We perform this investigation for Pulsar Timing Array experiments of different durations as well as ground-based and space-borne interferometric detectors.

Subject headings: early universe — gravitational waves — instrumentation: miscellaneous — methods: numerical

1. INTRODUCTION

Cosmic strings are one-dimensional topological defects of cosmological size, expected to form either during symmetry breaking phase transitions in the early Universe (field theory strings) (Kibble 1976) or at the end of inflation in brane-world scenarios (cosmic superstrings) (Sarangi & Tye 2002).

The energy scale of cosmic strings is defined by their linear energy density or tension, μ , usually referenced through the dimensionless quantity $G\mu/c^2$, where G is Newton's constant and c the speed of light. In the case of field theory strings, the tension is directly related to the energy scale η of the phase transition that created them, $\mu \sim \eta^2$ in natural units, $\hbar = c = k = 1$. In the case of cosmic superstrings, their tension is directly related to the fundamental string coupling g_s and the compactification or warping scales. Therefore, the detection, or at least the constraining of the cosmic string tension, provides a unique laboratory for physics at high energies.

A cosmic string network consists of infinite strings which stretch beyond our horizon and string loops (Vilenkin & Shellard 1994). After its creation, the network evolves along with the expansion of the Universe and is expected to settle into a scaling regime where all its fundamental properties scale along with the horizon radius $\sim t$, which is called the one-scale model. The scaling evolution of the network is attained through the creation of loops. When two cosmic strings intersect, they intercommute with a probability p and exchange partners, chopping off loops from the network (Shellard 1987; Jackson et al. 2005). In the one-scale model, loops are born with a size ℓ_b equal to a fraction of the particle horizon d_H at the time of their birth, $\ell_b(t) = \alpha d_H(t)$, where α is a constant. These loops subsequently decay by emitting all of their energy in various forms of radiation,

with the most dominant of them expected to be gravitational waves (GWs) (Vilenkin (1981); see, Vincent et al. (1997) for an alternative). The GW emission from all the loops created by the network creates a stochastic gravitational wave background (SGWB).

Recently, Sanidas et al. (2012) have studied in detail the properties of the cosmic string SGWB and set a conservative upper limit on the cosmic string tension, $G\mu/c^2 < 5.3 \times 10^{-7}$ for networks with $\alpha \geq 10^{-9}$, avoiding any assumption on the parameters describing the GW emission mechanism. Our result is approximately one order of magnitude weaker than the equivalent limit found by the Damour & Vilenkin (2005) analytic relation, $G\mu/c^2 < 1.2 \times 10^{-8}$ (van Haasteren et al. 2011, 2012), which is due to the strong assumptions made for the latter (see also discussion in Schlaer et al. (2012)).

As part of the common effort of the European Pulsar Timing Array (EPTA¹, Ferdman et al. (2010)) collaboration to detect GWs with pulsar timing, we present here an expansion of our previous work to evaluate the tension constraints that will be achieved by future Pulsar Timing Array (PTA) experiments of different durations and ground-based/space-borne interferometers. This not only allows us to predict future constraints, but the semi-analytic formulae we deduce can be used when the limits on $\Omega_{\text{gw}}h^2$ become available. First, we establish the parameter space accessible by each of these detectors. Then, we discuss how the exclusion curves on the parameter space evolve relative to $\Omega_{\text{gw}}h^2$. Using this information, we will evaluate the tension constraints as a function of $\Omega_{\text{gw}}h^2$ for a range of experiments. We will also derive semi-analytic formulae for ease of use in future investigations. Additionally, we discuss how the radiative efficiency parameter Γ , affects these constraints.

¹ <http://www.epta.eu.org>

2. CONSTRAINING THE STRING TENSION

2.1. *The cosmic string SGWB*

In the one-scale model, the basic parameters that determine the GW spectrum are: the cosmic string tension, $G\mu/c^2$; the birth scale of loops relative to the horizon, α ; and the intercommutation probability, p . In order to compute the SGWB, we also need to model the spectrum of radiation emitted by a cosmic string loop. This is quantified by: its spectral index q , with $q = 4/3$ for cusps and $q = 2$ for kinks (Vilenkin & Shellard 1994); a cut-off on the number of emission modes, $n_* = 1 \rightarrow \infty$, which is used to model the effects of gravitational backreaction (Caldwell et al. 1996); and the radiative efficiency $\Gamma \approx 50$, which describes the efficiency of the GW emission mechanism (Casper & Allen 1995). In Sanidas et al. (2012) we have described in detail the computation of the cosmic string SGWB which we will only briefly recap it here.

From the energy-momentum tensor for cosmic strings we find the energy lost into loops in order for the network to maintain scaling,

$$\frac{dE_{\text{loop,cr}}}{dt} = -V(t) \left[\dot{\rho}_{\infty}(t) + 2 \frac{\dot{a}(t)}{a(t)} \rho_{\infty}(t) (1 + \langle v^2 \rangle / c^2) \right], \quad (1)$$

where $\rho_{\infty}(t) = A\mu d_H^{-2}(t)c^2$ is the energy density of infinite strings, A is the number of infinite strings within the horizon, $\langle v^2 \rangle$ is the mean squared velocity of cosmic strings, $a(t)$ the scale factor and $V = a^3(t)$ is the computation volume. We have considered A and $\langle v^2 \rangle$ as fixed parameters, using their most recently published values (Blanco-Pillado et al. 2011), quoted in Table 1. Assuming that loops have a length $\ell_b(t) = \alpha d_H(t)$ when they are born, from Eq. (1) we can find the loop formation rate,

$$\frac{dN_{\text{loop}}}{dt} = \frac{2V(t)\rho_{\infty}(t)}{\mu\alpha d_H(t)c^2} \left[\frac{c}{d_H(t)} - \frac{\dot{a}(t)\langle v^2 \rangle}{a(t)c^2} \right], \quad (2)$$

where N_{loop} is the total number of loops within $V(t)$ created since the creation of the network at $t_f = t_{\text{Pl}}c^4/(G\mu)^2$, with t_{Pl} the Planck time. Since the rate of decay of length for loops is $\Gamma G\mu/c$, we are able to compute the number density $n(\ell, t)d\ell$ of loops with length between ℓ and $\ell + d\ell$ present at time t .

In our GW emission model, each loop emits into a series of harmonics n , with frequency

$$f_n = \frac{2nc}{\ell}, \quad (3)$$

and power $dE_{\text{gw,loop}}/dt = P_n G\mu^2 c$ with $P_n = \Gamma n^{-q} / \sum_{m=1}^{n_*} m^{-q}$. Then, using Eq. (3) and carefully redshifting the frequencies to the present time we can construct $n_j(f, t)$ that provides the number density of loops, which at the j th mode and at time t , emit GWs detected at frequency f . The computation of the energy density of GWs per logarithmic frequency interval $\Omega_{\text{gw}} h^2$, where $H_0 = 100h \text{ km s}^{-1} \text{ Mpc}^{-1}$ is the Hubble

parameter at the present time t_0 , is then given by

$$\Omega_{\text{gw}}(f) = \frac{2G\mu^2 c^2}{\rho_{\text{crit}} a^5(t_0) f} \sum_{j=1}^{n_*} j P_j \int_{t_f}^{t_0} a^5(t') n_j(f, t') dt', \quad (4)$$

where $\rho_{\text{crit}} = 3H_0^2 c^2 / 8\pi G$ is the critical energy density.

A correction has to be applied in Eq.(4) due to the annihilation of massive particles during the radiation era. When the temperature of the Universe, T , drops below a specific particle mass threshold, the relevant family becomes non-relativistic, changing the number of relativistic degrees of freedom, g_* . This will result in a faster expansion of the Universe every time such a mass threshold is crossed, affecting the value of $a(t)$ (Kolb & Turner 1990). Although these changes will not significantly affect the evolution of the cosmic string network, which will quickly adapt to the new expansion rate and converge to its scaling evolution, they will have a significant effect on the energy density of the GWs emitted by the network.

These effects can be included with the use of a multiplicative factor for ρ_{gw} , and therefore $\Omega_{\text{gw}} h^2$, which has the form $(g_*/g'_*)^{1/3}$, where g'_* and g_* are the relativistic degrees of freedom before and after the transition, and acts to decrease the amplitude of the SGWB (Bennett 1986; Caldwell & Allen 1992; Binétruy et al. 2012). This correction is applied at time $t_{\text{cor}} = (32\pi G\rho/3)^{-1/2}$, where $\rho = \pi^2 g_* T^4 / 30$ and its effects are observed at a frequency $f_{\text{cor}} \approx 2a(t_{\text{cor}})c[f_r \alpha d_H(t_{\text{cor}})a(t_0)]^{-1}$, which depends strongly on α . PTAs, probing nHz GWs, are not significantly affected by these corrections, and that only in the case where α is large. These corrections were not considered in Sanidas et al. (2012), but this does not affect the robustness of the results presented in the aforementioned paper. However, when considering GW detectors operating at the Hz and mHz bands significant corrections are expected. We have computed these corrections for every particle in the Standard Model using the mass values in Beringer et al. (2012) and incorporated them to the computed spectra. In Fig. 1 we present a typical cosmic string GW spectrum for $\alpha = 0.1$ with the characteristic peak and flat part originating from the loop populations in the matter and radiation eras respectively, along with the corrections to the spectrum due to particle annihilation.

2.2. *Exclusion Curves*

The computation of the tension exclusion curves and upper bounds for a SGWB limit is done using the procedure described in Sanidas et al. (2012). First, we compute the GW spectra of cosmic string models covering all the accessible parameter space. Second, we find which configurations are compliant with the SGWB limit, both in terms of amplitude and assuming a flat local slope². Finally, we plot these configurations in the $G\mu - \alpha$ parameter space and the maximum tension allowed for a given $\Omega_{\text{gw}} h^2$ limit will provide the tension upper limit.

For a particular experiment, it is essential to determine the range of α values which are accessible to it. The

² Since we are only considering projected constraints by future experiments, an assumption for the spectral slope is necessary. We will discuss our choice later.

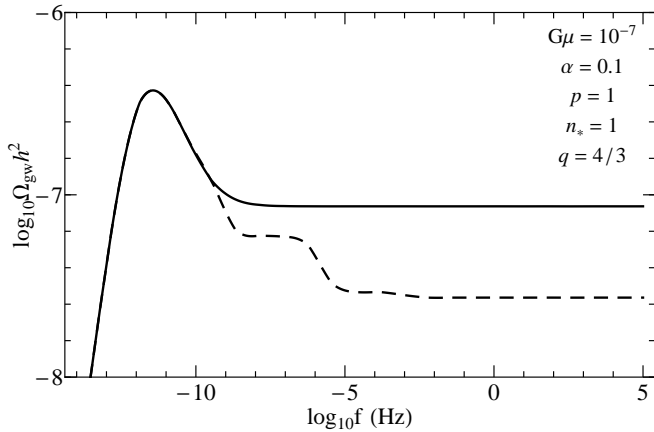


FIG. 1.— The SGWB of a cosmic string network before (solid line) and after (dashed line) the particle annihilation corrections are applied.

SGWB of cosmic strings can span a wide range of frequencies, from below the nHz regime to beyond a THz, which depends on the size of the loops created by the network. The minimum frequency f_{\min} of the SGWB is provided by the first emission mode of the loops which are born at t_0 , and hence $\alpha_{\min} = f_{\min} f_{\text{r}} d_{\text{H}}(t_0)/2c$.

In this work, we will not treat the GW detectors as broadband, but instead we will designate each one a fiducial frequency; the one at which maximum sensitivity is achieved. For ground-based interferometers (hereafter, “Hz-detectors”) and space-borne interferometers (hereafter, “mHz-detectors”), we have assumed fiducial frequencies of $f = 100$ Hz and $f = 0.01$ Hz respectively. For PTA experiments, the fiducial frequency is the inverse of the elapsed time over which observations were taken: $f = 6.3$ nHz, $f = 3.2$ nHz and $f = 1.6$ nHz for 5-, 10-, and 20-year PTA experiments respectively. They can only detect GW emission for $\alpha \geq \alpha_{\min}$, where $\log_{10} \alpha_{\min} = -9.5$ for a 5-year PTA, $\log_{10} \alpha_{\min} = -9.2$ for a 10-year PTA, $\log_{10} \alpha_{\min} = -8.9$ for a 20-year PTA, $\log_{10} \alpha_{\min} = -15.7$ for mHz-detectors and $\log_{10} \alpha_{\min} = -19.7$ for Hz-detectors. Of course, real detectors are broadband and can observe at higher frequencies than the one that maximum sensitivity is achieved, but, since they are typically only sensitive for a few orders of magnitude in frequency, α_{\min} provides a useful rule-of-thumb.

In Fig. 2 we present the exclusion curves for networks with $p = 1$ for three projected limits on $\Omega_{\text{gw}} h^2$ at $f = 6.3$ nHz and $f = 100$ Hz. In the case of PTAs (upper panel), for $\Omega_{\text{gw}} h^2 \gtrsim 10^{-10}$, the upper limit on $G\mu/c^2$ is provided by the peak in the mid- α region. The rise in the exclusion curve for $\alpha \sim \alpha_{\min}$ is expected, since in that region the detector probes the spectrum at frequencies lower than the peak frequency, with higher values of $G\mu/c^2$ required for a fixed $\Omega_{\text{gw}} h^2$. For $\Omega_{\text{gw}} h^2 \ll 10^{-10}$, the characteristic peak disappears and the upper limit on the tension is provided by the models with $\alpha = \alpha_{\min}$.

The $\Omega_{\text{gw}} h^2$ value at the low frequency cut-off is provided by the loops which are born at the present time and therefore, it will not be stochastic. In reality, the SGWB is expected to start from a frequency $f \gtrsim f_{\min}$, where the individual loop emission becomes unresolvable, reducing the height of the secondary peak and overestimating the tension constraints for $\Omega_{\text{gw}} h^2 \lesssim 10^{-10}$. However, since in

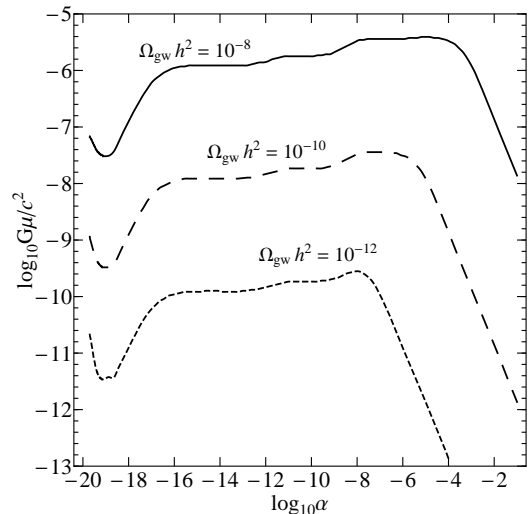
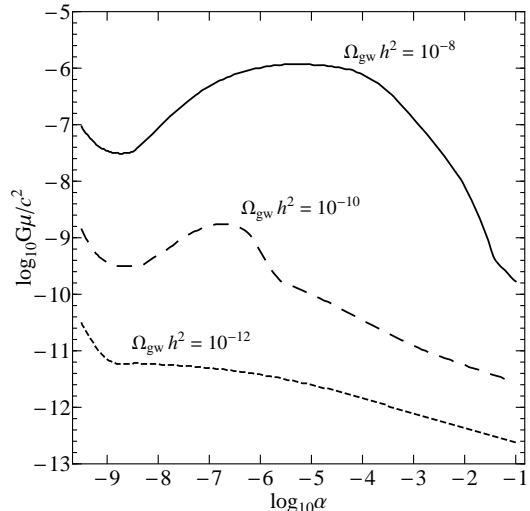


FIG. 2.— Exclusion limits for cosmic string networks with $p = 1$ and various values for the upper limit on $\Omega_{\text{gw}} h^2$ at $f = 6.3$ nHz (upper panel) and $f = 100$ Hz (lower panel).

that case the spectrum has a positive slope, our assumption for a flat spectrum leads to an underestimation of the tension constraints. These two effects are expected to be similar and cancel out, preserving the robustness of our results.

The shape of the exclusion curves for Hz- and mHz-detectors exhibit a much less prominent mid- α peak (see, for example, Fig. 2, lower panel). The whole mid- α region would be flat if we had not considered the massive particle annihilation corrections; a result of the fact that such detectors probe only the flat part of the spectrum originating from the radiation era. Moreover, the upper limits on the tension are always provided by the mid- α peak since the peak created by the networks with $\alpha \sim \alpha_{\min}$ never gets higher.

3. PROJECTED CONSTRAINTS

We computed the spectra for ~ 32000 different parameter sets ($\sim 1.3 \times 10^5$ CPU hours), using an updated version of the code used in Sanidas et al. (2012). Most changes concern numerical accuracy improvements and the use of the recently published values for the infinite

TABLE 1
PARAMETER VALUES
USED/INVESTIGATED IN THIS WORK.

Quantity	Value(s)
A (radiation era)	45
A (matter era)	35
$\langle v^2 \rangle / c^2$ (radiation era)	0.40
$\langle v^2 \rangle / c^2$ (matter era)	0.35
f_r	0.71
$G\mu/c^2$	$[10^{-13}, 10^{-4}]$
α	$[10^{-19.7}, 0.1]$
q	$-4/3, -2$
n_*	$1, 10^4$
Γ	$50, [10, 100]$

string parameters from Blanco-Pillado et al. (2011). A list of all these parameter values along with the value ranges we covered for the fundamental cosmic string model parameters is presented in Table 1. It is only necessary to use a small number of spectral parameters, since the tension constraints for any α in the $G\mu/c^2 - \alpha$ parameter space will always be provided by the exclusion curves of either the $q = 4/3$, $n_* = 1$ or the $q = 4/3$, $n_* = 10^4$ models as shown in Sanidas et al. (2012). Additionally, we only considered networks with $p = 1$ since the final results can be easily rescaled for networks with $p \neq 1$. For the core results of this paper we used $\Gamma = 50$ (Casper & Allen 1995).

We have investigated SGWB amplitudes in the range $\Omega_{\text{gw}} h^2 \in [10^{-12.5}, 10^{-7}]$, with $\Delta \log_{10}(\Omega_{\text{gw}} h^2) = 0.1$. For each value for $\Omega_{\text{gw}} h^2$, we have computed the exclusion curves as a function of α and located the highest possible $G\mu/c^2$ value. In Fig. 3 (left panel) we present the projected tension constraints as a function of $\Omega_{\text{gw}} h^2$.

For PTAs, the constraints on the tension are almost independent of the frequency of maximum sensitivity except in the region $10^{-10} \lesssim \Omega_{\text{gw}} h^2 \lesssim 10^{-9}$. Longer duration experiments are preferred in that region³, which is the expected sensitivity to the SGWB for LEAP (Kramer & Stappers 2010). The change in the slope of the curve at $\Omega_{\text{gw}} h^2 \sim 10^{-10}$ signifies the point at which the tension upper limit is no longer provided by the mid- α peak but instead from the $\alpha \sim \alpha_{\text{min}}$ models. The mHz-detectors will provide weaker constraints on the tension for all $\Omega_{\text{gw}} h^2$ values investigated. The same applies for Hz-detector, which will provide weaker constraints than both PTAs and mHz-experiments.

The relatively simple origin of the constraint curves makes it possible to describe them with fitting formulae $G\mu(\Omega_{\text{gw}} h^2)/c^2$. This will allow any future constraint on $\Omega_{\text{gw}} h^2$ by any experiment operating in the relevant frequency range to be directly connected to a robust constraint on the string tension. Using least squares fitting and setting $x = \log_{10}(\Omega_{\text{gw}} h^2)$, we find that:

³ Longer duration experiments will eventually collect more data and set more stringent constraints on $\Omega_{\text{gw}} h^2$ than the shorter duration ones. However, if two such experiments manage to set the same constraint on $\Omega_{\text{gw}} h^2$, the longer duration one will provide better constraints on the string tension in that region. The better performance of longer duration experiments stems from the lower frequency that they probe with maximum sensitivity, placing them “deeper” in the high amplitude, matter era peak of the cosmic string GW spectrum.

For 5-year PTA experiments,

$$\log_{10}(G\mu/c^2) \leq \begin{cases} 0.0959x^3 + 2.292x^2 + 19.23x + 50.31 \\ \text{for } -10 < x \leq -7, \\ 0.0917x^2 + 2.85x + 10.5 \\ \text{for } -12.5 \leq x \leq -10. \end{cases} \quad (5)$$

For 10-year PTA experiments,

$$\log_{10}(G\mu/c^2) = \begin{cases} 0.126x^3 + 2.972x^2 + 24.36x + 63.22 \\ \text{for } -9.8 < x \leq -7, \\ 0.0794x^2 + 2.53x + 8.52 \\ \text{for } -12.5 \leq x \leq -9.8. \end{cases} \quad (6)$$

For 20-year PTA experiments,

$$\log_{10}(G\mu/c^2) = \begin{cases} 0.1565x^3 + 3.629x^2 + 29.05x + 74.31 \\ \text{for } -9.5 < x \leq -7, \\ 0.074x^2 + 2.37x + 7.46 \\ \text{for } -12.5 \leq x \leq -9.5. \end{cases} \quad (7)$$

For mHz-detectors,

$$\log_{10}(G\mu/c^2) = 1.09x + 3.16 \text{ for } -12.5 \leq x \leq -7. \quad (8)$$

For Hz-detectors,

$$\log_{10}(G\mu/c^2) = 1.03x + 2.83 \text{ for } -12.5 \leq x \leq -7. \quad (9)$$

These formulae can be easily adapted to describe cosmic string networks with $p \neq 1$. In Sanidas et al. (2012) we have pointed out that a non-zero intercommutation probability only rescales the GW spectrum, $\Omega_{\text{gw}} h^2 \propto p^{-k}$, where k is an index describing how the intercommutation probability affects the population statistics of infinite strings, and whose value is discussed in Sakellariadou (2005) and Avgoustidis & Shellard (2005, 2006). Therefore, Eqs. (5), (6), (7), (8) and (9) can provide constraints for any possible combination of p simply by multiplying the polynomials with p^{-k} .

Additionally, we have investigated the effects of varying Γ on the tension constraints. The value of Γ depends on the trajectory of each loop and is expected to be in the range $\sim 50 - 100$ (Allen & Casper 1994; Casper & Allen 1995; Bohé 2011; Copi & Vachaspati 2011). We have computed the tension constraints for networks with $\Gamma \in [10, 100]$ and we present some typical results in the right panel of Fig. 3. In the case of Hz- and mHz detectors the effects of varying Γ do not significantly change the tension constraints. The same holds true for PTAs, except in the region $10^{-10.5} \lesssim \Omega_{\text{gw}} h^2 \lesssim 10^{-9}$ where low values of Γ are equivalent to decreasing the frequency of maximum sensitivity.

We will conclude this section by discussing the consequences of our assumption of a locally flat spectrum. For Hz- and mHz-detectors, this assumption holds true since these detectors probe the flat part of the spectrum for most of the $G\mu - \alpha$ parameter space. In the case of PTAs, the slope will be negative when $\Omega_{\text{gw}} h^2 \gtrsim 10^{-10}$ (upper limit provided by the mid- α peak) and positive

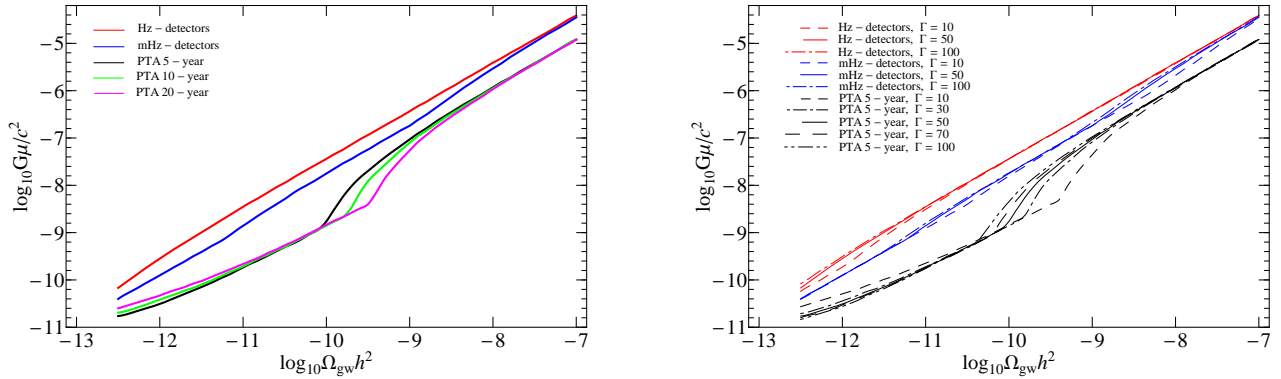


FIG. 3.— Cosmic string tension upper limits for networks with $p = 1$ as a function of $\Omega_{\text{gw}}h^2$ for various GW detection experiments (left panel) and the effects of varying Γ (right panel).

when $\Omega_{\text{gw}}h^2 \lesssim 10^{-10}$ (upper limit provided by the peak at $\alpha \sim \alpha_{\text{min}}$). In the first case, the flat spectrum assumption will lead to an underestimation of the constraint. For example, the EPTA limit on the string tension of Sanidas et al. (2012) will provide a hint on the expected discrepancy. Reworking that analysis under the assumption of a flat spectrum we find $G\mu/c^2 < 5.6 \times 10^{-7}$ whereas the limit we acquired using the extra slope information was $G\mu/c^2 < 5.3 \times 10^{-7}$, a 5.6% discrepancy. We anticipate that the projected constraints in the whole range where $\Omega_{\text{gw}}h^2 \gtrsim 10^{-10}$ will be higher by a similar percentage, something that does not affect the robustness of our approach since we are interested in conservative constraints. In the case where, $\Omega_{\text{gw}}h^2 \lesssim 10^{-10}$ the constraints are expected to be overestimated by a similar percentage. However, expect that this will be canceled by a similar order underestimation of the constraints in this region due to the assumption of the stochastic nature of the background at f_{min} , as discussed in Sec. 2.2.

4. DISCUSSION

In this paper, we have presented fitting formulae for the upper limits on the cosmic string tension which can be used in future GW detection experiments. These constraints are free of any assumption on model parameters within the one-scale model. These formulae provide a conservative alternative to the approach discussed in Damour & Vilenkin (2005) which is based on cusp emission and an approximate loop number density, assumptions which are much stronger.

The GW spectrum of cosmic strings, being extremely broadband is potentially accessed by every GW detection experiment, with each of them probing bands with

different properties. PTAs, probing the high amplitude matter era peak of the spectrum for most cosmic string model parameter combinations and only partially suffering from the massive particle annihilation corrections in the case of large loops, provide an excellent tool to detect strings, or at least, set the most stringent constraints on their tension. On the other side, ground-based interferometers probe a much wider area of the parameter space ($\alpha_{\text{min}} \approx 10^{-20}$) making them the only tool able to detect emission from very small loops, and they are not sensitive to the, unknown, details of the radiation spectrum (q and n_*). Space-borne interferometers, operating in a frequency range between PTAs and ground-based interferometers, share advantages and disadvantages from both.

PTAs already set the most stringent constraints on the amplitude of the SGWB when compared to LIGO, and Advanced LIGO which is expected to become operational in 2015 will achieve a similar performance (Harry & the LIGO Scientific Collaboration 2010). The further increase in the sensitivity of PTAs expected in the near future (LEAP is expected to set upper limits on $\Omega_{\text{gw}}h^2 \lesssim 10^{-10}$), will lead to constraints on $G\mu/c^2 \lesssim 2 \times 10^{-9}$, with a SKA⁴-scale PTA experiment improving this by two orders of magnitude.

5. ACKNOWLEDGEMENTS

The authors would like to thank Michael Kramer, Mark Hindmarsh, and acknowledge the support of the colleagues in the EPTA during the preparation of this paper.

REFERENCES

- Allen, B., & Casper, P. 1994, Phys. Rev. D, 50, 2496
 Avgoustidis, A., & Shellard, E. P. 2005, Phys. Rev. D, 71, 123513
 Avgoustidis, A., & Shellard, E. P. S. 2006, Phys. Rev. D, 73, 041301
 Bennett, D. P. 1986, Phys. Rev. D, 34, 3592
 Beringer, J., et al. 2012, Phys. Rev. D, 86, 010001
 Binétruy, P., Bohé, A., Caprini, C., & Dufaux, J.-F. 2012, J. Cosmol. Astropart. Phys., 6, 27
 Blanco-Pillado, J. J., Olum, K. D., & Shlaer, B. 2011, Phys. Rev. D, 83, 083514
 Bohé, A. 2011, Phys. Rev. D, 84, 065016
 Caldwell, R. R., & Allen, B. 1992, Phys. Rev. D, 45, 3447
 Caldwell, R. R., Battye, R. A., & Shellard, E. P. S. 1996, Phys. Rev. D, 54, 7146
 Casper, P., & Allen, B. 1995, Phys. Rev. D, 52, 4337
 Copi, C. J., & Vachaspati, T. 2011, Phys. Rev. D, 83, 023529
 Damour, T., & Vilenkin, A. 2005, Phys. Rev. D, 71, 063510
 Ferdman, R. D., et al. 2010, Class. Quant Grav., 27, 084014
 Harry, G. M., & the LIGO Scientific Collaboration. 2010, Class. Quant Grav., 27, 084006
 Jackson, M. G., Jones, N. T., & Polchinski, J. 2005, J. High Energy Phys., 10, 013
 Kibble, T. W. B. 1976, J. Phys. A: Math. Gen., 9, 1387
 Kolb, E. W., & Turner, M. S. 1990, The Early Universe. (Addison-Wesley)
 Kramer, M., & Stappers, B. 2010, Proc. Sci. ISKAF2010

⁴ <http://www.skatelescope.org>

- Sakellariadou, M. 2005, *J. Cosmol. Astropart. Phys.*, 04, 003
- Sanidas, S. A., Battye, R. A., & Stappers, B. W. 2012, *Phys. Rev. D*, 85, 122003
- Sarangi, S., & Tye, S.-H. H. 2002, *Phys. Lett. B*, 536, 185
- Shellard, E. P. S. 1987, *Nucl. Phys. B*, 283, 624
- Shlaer, B., Vilenkin, A., & Loeb, A. 2012, *J. Cosmol. Astropart. Phys.*, 5, 26
- van Haasteren, R., et al. 2011, *MNRAS*, 414, 3117
- . 2012, *MNRAS*, 425, 1597
- Vilenkin, A. 1981, *Phys. Lett. B*, 107, 47
- Vilenkin, A., & Shellard, E. P. S. 1994, *Cosmic Strings and Other Topological Defects* (Cambridge: Cambridge University Press)
- Vincent, G. R., Hindmarsh, M., & Sakellariadou, M. 1997, *Phys. Rev. D*, 56, 637